Article

Quantum chemical simulation of epirubicin interaction with fullerene and carbon graphene-like plane

B. M. Gorelov, O. V. Khora, E. M. Demianenko[*]**, N. A. Havryliuk, A. G. Grebenyuk, V. V. Lobanov**

Chuiko Institute of Surface Chemistry of National Academy of Sciences of Ukraine, 17 General Naumov Str., 03164 Kyiv, Ukraine
* Corresponding author: E. M. Demianenko, demianenko_en@ukr.net

Abstract: Creation of new "targeted delivery" drugs is one of priority areas of pharmacology and is especially true for oncology. Medicinal substances, in particular those of anthracycline series, immobilized on the surface of nanosized carriers for the targeted delivery of drugs to target organs or target tissues, allow creating an optimal concentration of the drug in the area of therapeutic effect. The latter significantly reduces systemic toxicity by decreasing the total dose and longer retention in the lesion, as well as increasing the solubility and bioavailability of drugs. Ones of promising drug delivery nanosystems are carbon materials, in particular, fullerene (C_{60}) and pristine or modified graphene. The feature of carbon systems, in contrast to organic and dielectric transport systems, is their high conductivity and the dependence of the interaction energy between atoms of transporters and drugs on their charge state. To date, the specifics of the interaction of epirubicin with a graphene-like plane (GP) and fullerene at the atomic level remain poorly understood. Therefore, the energy parameters of the interaction of GP and C_{60} with epirubicin in various protolytic forms, which reveal at different pH values of the aqueous medium, were studied using quantum chemistry methods. Calculations were carried out using the MOPAC2016 program and the PM6-D3H4X method, in which, along with hydrogen bonds, the dispersion interactions are taken into account. Based on the analysis of the results of quantum chemical studies, the thermodynamic probability of the epirubicin adsorption process on GP is predicted in the entire pH range of the aqueous medium, as evidenced by the negative values of interaction enthalpies in all four cases. It has been found that epirubicin (protonated form) will have the greatest adsorption both on the graphene plane (−209.1 kJ/mol) and upon interaction with the fullerene molecule (−121.3 kJ/mol).

Keywords: epirubicin; fullerene; graphene-like plane; cluster approximation; semi-empirical research methods

1. Introduction

Antitumor drugs of anthracycline series, such as doxorubicin and epirubicin, inhibit the growth and reproduction of cells. Cells of malignant neoplasms, which divide rapidly, are particularly sensitive to the action of such drugs. Herein, the functionality of normal cells of a number of body systems is suppressed. The common side effects are hair loss (alopecia), vomiting, inhibition of bone marrow function, inflammation of the inner part of the oral cavity, death of epithelial tissues at the injection site, as well as high cardiotoxicity [1–5].

The cardiotoxic effect of anthracyclines is often the main limiting factor for highly effective cytostatic chemotherapy [6] and is a good reason for stopping treatment even before a clear antitumor effect is obtained. The danger of heart damage lies in the high frequency of their development, the difficulties of diagnosis, their long latent course, the possibility of occurrence not only during the period of treatment, but also many years after ending of anticancer chemotherapy [7]. Myocardial cell damage leads to violations of the ultrastructure and functional failure of the heart muscle. Metabolic damage to cardiomyocytes caused by exposure to toxic anthracyclines causes the development of oxidative stress [8], which leads to apoptosis (death) of cells and necrosis of heart tissues.

Currently, toxic damage to the myocardium by anthracyclines and its prevention with the help of pharmacological agents remains an unsolved problem in oncology [9]. Therefore, the search for medicinal substances of natural and synthetic origin with optimal pharmacodynamic and pharmacokinetic parameters for the prevention and correction of structural and functional disorders in myocardial tissue, under conditions of chronic intoxication with antitumor drugs, can solve one of the urgent problems of modern medicine.

However, medicinal substances immobilized on the surface of nanosized carriers for the targeted delivery of drugs to target organs or target tissues allow creating an optimal concentration of the medicinal substance in the area of the therapeutic effect [10,11]. This significantly reduces systemic toxicity due to the reduction of the total dose and longer retention of the active substance in the lesion. Ideally, carriers also increase their solubility and bioavailability [12,13]. Thus, the creation of new "targeted delivery" drugs is one of the priority areas of pharmacology and, in particular, of oncology [14,15].

One of the promising auxiliary substances are nanocarbon materials, in particular, fullerene (C_{60}) and original and modified graphene [16–18]. The paper [19] analyzed the possibility of using C_{60} and C_{70} fullerenes as a neutral means of drug delivery to the affected area. It has been found that fullerenes, having low toxicity, retain a unique ability for chemical modification, namely, the addition of functional groups with double bonds, the introduction of atoms and entire clusters into the carbon sphere, as well as the formation of new compounds by replacing one carbon atom with an atom of another chemical element [20]. The high reactivity of the surface of fullerenes contributes to the fixation of anthracyclines, the main structure of which is a tetracyclic molecule with an anthraquinone skeleton connected to a sugar fragment by a glycosidic bond. Since the spatial dimensions of modified molecules are in the nanometer range, when injected into human blood, they can pass through the capillaries of the circulatory system. High permeability makes fullerenes promising carriers of dosage forms for targeted delivery [21]. In work [22], the properties of oncopreparations based on nanocomposites of doxorubicin with graphene and its oxide were predicted using quantum chemistry methods.

Herein, creating an increased drug concentration near a diseased organ enhances the penetrating probability of immobilized drug within diseased cells, but does not guarantee successful treatment of the organ. Important therapeutic procedures are the passage of nanosized carbon carriers with an immobilized drug, or separately, through the cell membrane within the intracellular medium (the cytoplasm) of the diseased organ and the subsequent unfastening process of drugs or its atomic fragments from transporter and their sticking to substances localized in the cell nucleus, in particular, DNA molecules. During the sticking process the interaction of atomic complexes of drug and DNA molecules is accompanied by variations in the charge and structural states of formed atomic complexes of dosage form with nuclear substances, what may produce a therapeutic effect at the molecular level.

In addition, the detachment process of dosage forms from the carrier and their sticking to the DNA molecule is supported by thermal and charge fluctuations in the intracellular environment, stimulated by heart contractions. Therefore, the detachment energy of the dosage form from the carrier and their sticking energy to DNA molecules may be of the order of the physical adsorption energy and does not excess the chemical adsorption minimal value, i.e., $E_d < 40$ kJ/mol. Since the energy of thermal vibrations is $\sim kT$, where k is Boltzmann's constant, T is the temperature of the intracellular medium, at $T \sim 37$ °C their energy contribution to the detachment and sticking processes is about ~ 2.5 kJ/mol.

Besides, the accumulation of charged drug atomic fragments or the excess of drug molecules not involved in the therapeutic process in the intracellular environment may lead to the cytotoxicity development [23]. Therefore, the drug delivery carriers must have the sufficient probability for exit and removal from the intracellular environment the drug atomic fragments and excess molecules not involved in the therapeutic process.

Currently, along with doxorubicin, its enantiomer, epirubicin, is used in medical practice, which has identical pharmacological activity, but exhibits much lower cardiotoxic side effects [24,25]. Epirubicin is characterized by the following dissociation constants: $pK_{a1} = 8.5$; $pK_{a2} = 10.75$; $pK_{a3} = 11.33$ [26]. Therefore, in an aqueous solution, depending on the pH, epirubicin can be in protonated (H_3A^+), uncharged (H_2A) and deprotonated (HA^-, A^{2-}) forms, which are slightly different in structure and, as a result, have different capability to interact with graphene and fullerene.

After introducing into the bloodstream of a living body, nanosized carbon carriers with immobilized epirubicin move in a slightly alkaline environment with pH of 7.35–7.45 before contact with the cells of the diseased organ. Passing through the cell membrane, they enter within the intracellular weakly acidic environment with pH < 7. Thus, when moving from the extracellular to the intracellular environment, the charge state of the epirubicin and medium, where the drug is localized, may change abruptly. The variation in the cytoplasm pH value promotes the detachment of sorbed atomic groups on epirubicin molecules into the intracellular medium. The such process may lead, on the one hand, to a reduction in the medium acidity, and yield an inhibitory effect, in particular, on the cancer cells, and, on the other hand, change the binding energy value among atoms of the drug

and carbon carriers, and the intensity of intracellular transformations.

Assuming that during delivery of epirubicin molecules immobilized on nanosized transporters, such as the graphene layer and fullerenes, their charge state changes in an environment with different pH values, it is possible to estimate variations in the binding energy of the drug forms with the carbon carriers.

To date, the specifics of the interaction of epirubicin with fullerene and a graphene-like plane (GP) at the atomic level remain poorly understood. Therefore, the interaction of GP and C_{60} intermolecular complexes with epirubicin in various protolithic forms, which exist in the aqueous mediums with different pH values, were modeled by quantum chemistry methods and their energy parameters were calculated.

2. Objects and calculation methods

According to experimental and theoretical data [27–29], the epirubicin molecule has five proton-donating hydroxyl groups in the tetracyclic structure of the anthraquinone framework, which is connected by a glycosidic bond to one proton-accepting amino sugar fragment (**Figure 1a**). Therefore, the protonated form of epirubicin is formed as a result of protonation of the amino group (**Figure 1b**).
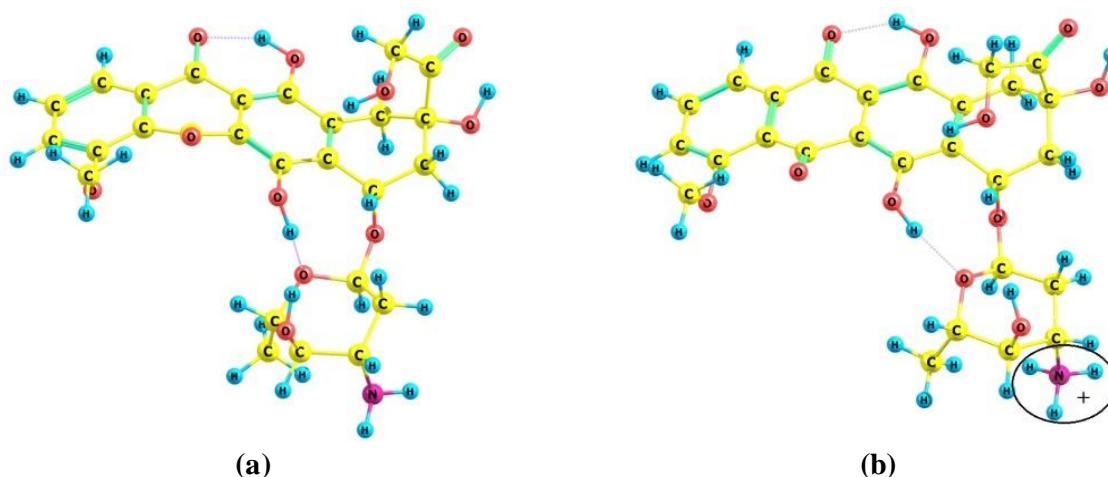

(a)   **(b)**

Figure 1. (a) Uncharged; and **(b)** protonated forms of epirubicin.

To elucidate which of the five hydroxyl groups of the epirubicin molecule has the highest proton-donating capacity, five epirubicin anions were optimized, each of which had one deprotonated hydroxyl group (**Figure 2**). It should be noted that when trying to localize the anion by detaching a proton from the hydroxyl group of the amino sugar fragment, during optimization, the proton moves from the hydroxyl group closest to it (**Figure 2d**). This indicates that the proton-donating ability of the hydroxyl group of the amino sugar fragment is the lowest.
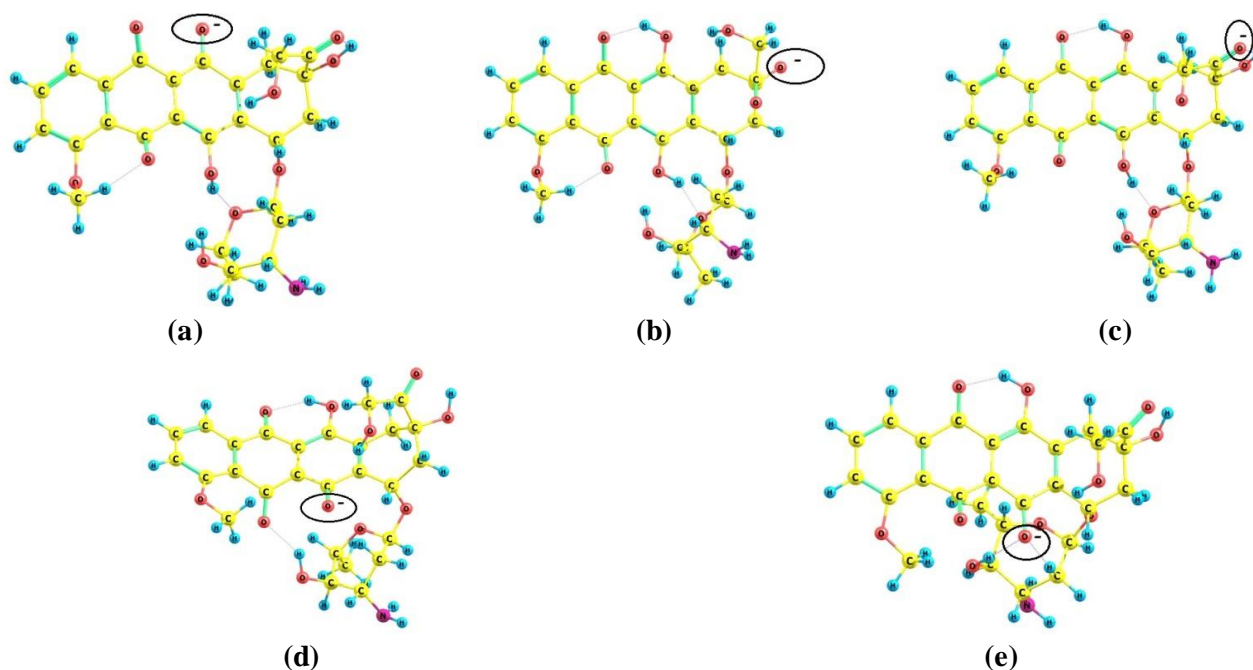
Figure 2. Possible equilibrium structures of the singly charged epirubicin anions and their total energies (here and in the future, the value of the total energy is given in kJ/mol) **(a)** −682649.9008; **(b)** −682582.1561; **(c)** −682483.2843; **(d)** −682725.299; **(e)** −682748.1516.

To establish the structure of the doubly deprotonated anion, four possible structures were optimized (**Figure 3**) by successive removal of a proton from the remaining four hydroxyl groups in the monoanion, which is shown in **Figure 2d**. According to the results of the analysis of the total energies of these dianions, it was found that the smallest value, and therefore the most probable, is the dianion depicted in **Figure 3a**.

Comparing the total energies of monoanions of epirubicin, it was found that the anion shown in **Figure 2e** has the deprotonated hydroxyl group located in the anthraquinone fragment, and the lowest total energy value. Therefore the proton-donating capacity of such hydroxyl group is the highest and it will be the first to dissociate in an aqueous solution. Note, in the future the epirubicin structure of shown in **Figure 2d** will be used as the HA- anion model.
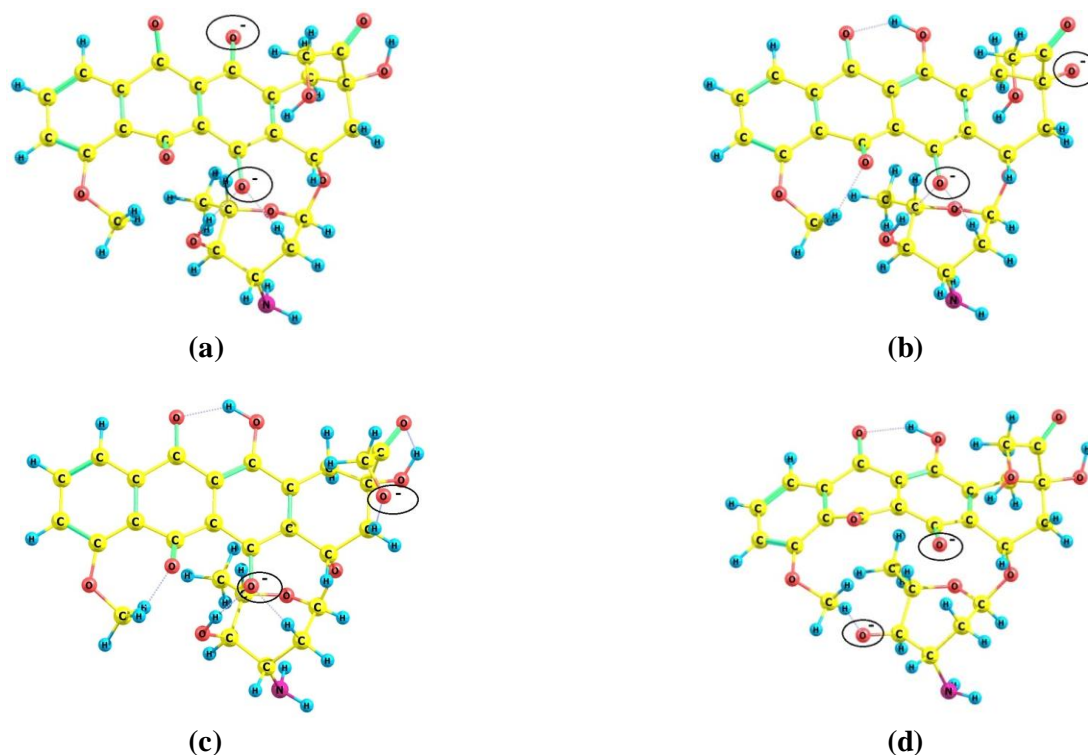
Figure 3. Equilibrium structures of doubly charged epirubicin anions and their total energies **(a)** −682649.9008; **(b)** −682582.1561; **(c)** −682483.2843; **(d)** −682525.299.

The smallest C_{60} molecule was chosen as the fullerene model, which is a sphere with a diameter of 7.13 Å (**Figure 4a**), which contains 60 equivalent carbon atoms, each of which is connected to three other covalent bonds, forming pentagons and hexagons on the surfaces. The $C = C$ bond lengths are 1.38 Å, and the $C - C$ bond lengths are 1.46 Å, respectively, which are confirmed by experimental and theoretical studies described in the literature, since the fullerene structure has been precisely established by experimental methods and studied in detail by theoretical methods [30,31].

A graphene-like plane commensurate with the epirubicin molecule (maximum length 12.2 Å, width 10.8 Å) was chosen as the graphene model. Its gross composition is $C_{54}H_{18}$ and contains 19 condensed benzene nuclei [32]. The graphene-like plane has a symmetrical structure (**Figure 4b**), with a length of 14.2 Å.
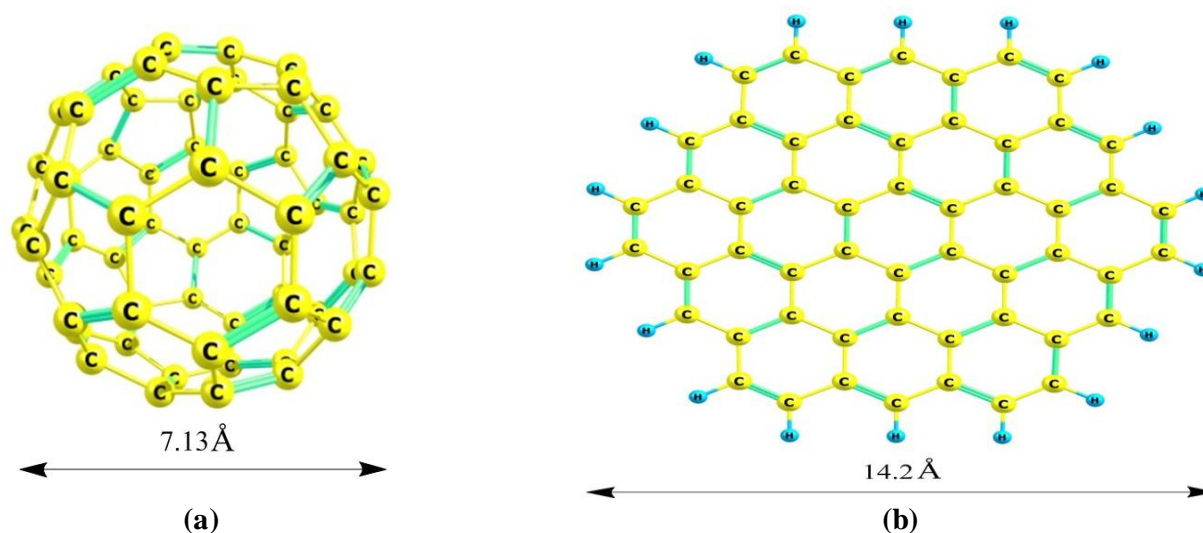
Figure 4. Equilibrium spatial structure of (a) the C_{60} fullerene molecule; and (b) the $C_{54}H_{18}$ graphene-like plane.

Calculations were performed using the MOPAC2016 program [33] and the PM6-D3H4X method [34–36], which takes into account the influence of hydrogen bonds and dispersion interactions. The enthalpy of adsorption was considered as the thermal effect (ΔH_{298}) of the interaction reaction of the epirubicin molecule (A) and GP or C_{60} (B) with the formation of an intermolecular complex (A···B) and according to the reaction

$$A + B \rightarrow A\cdots B$$
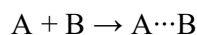
and calculated according to the formula:

$$\Delta H_{298} = H_{298}(A\cdots B) - [H_{298}(A) + H_{298}(B)],$$

де $H_{298}(A\cdots B)$—the enthalpy of formation of the intermolecular complex, $H_{298}(A)$—epirubicin, $H_{298}(B)$—GP or C_{60}, respectively, was calculated.

3. Results and their discussion

To begin with, the interaction of epirubicin with the fullerene molecule was investigated. Equilibrium structures of the most likely intermolecular complexes of C_{60} with epirubicin in various protolithic forms were found (**Figure 5**), the structure of which is given above (**Figures 2** and **3**). In particular, in **Figure 5** the intermolecular complex of the fullerene molecule with the protonated form of epirubicin is depicted. It can be seen that the acraquinone framework of epirubicin cation is significantly deformed, compared to the original one (**Figure 1b**) due to interaction with fullerene. At the same time, its protonated amino group is oriented towards the fullerene molecule. The enthalpy of this interaction has a negative value and is −121.3 kJ/mol, which indicates the thermodynamic probability of this process.

Next, the interaction of fullerene with the neutral epirubicin molecule is considered. As can be seen from **Figure 5b**, the epirubicin molecule due to interaction with fullerene is less deformed compared to its protonated form. ΔH_{298} of the interaction is much smaller compared to the similar value of the previous case and is only 38.5 kJ/mol (see **Table 1**).
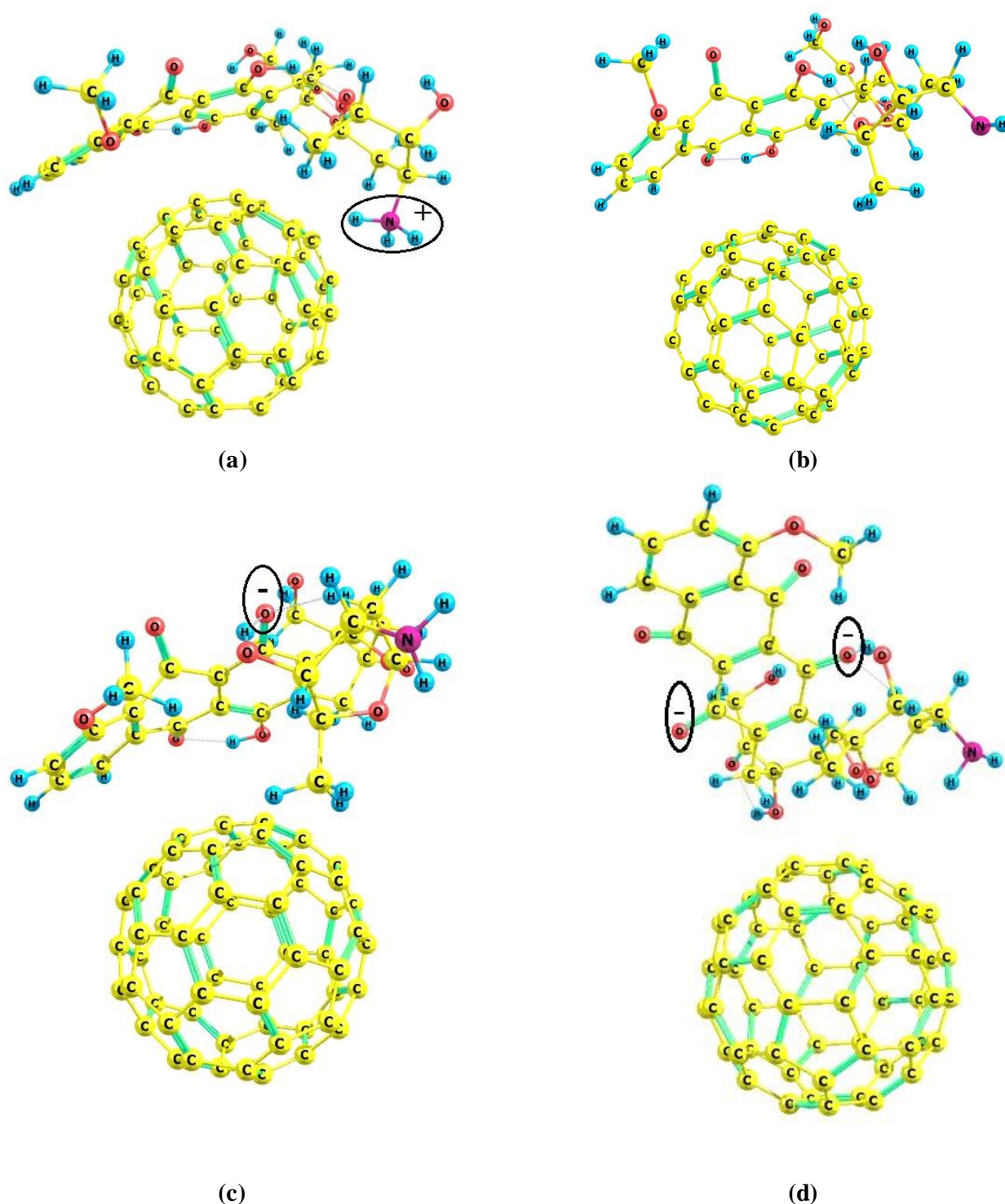
(a)

(b)

(c)

(d)

Figure 5. Equilibrium geometry of intermolecular complexes of the fullerene molecule with protolytic forms of epirubicin: **(a)** protonated; **(b)** neutral epirubicin molecule; **(c)** monodeprotonated; and **(d)** deprotonated.

As can be seen from **Figure 5c**, the structure of this intermolecular complex of epirubicin monoanion with a fullerene molecule is similar to the complex with a neutral epirubicin molecule. In particular, in both complexes the methyl group of the amino sugar fragment of epirubicin is oriented toward the fullerene molecule, while the amino group is oriented away from the C_{60} molecule. The interaction enthalpy is

slightly higher for the case with the epirubicin monoanion compared to the neutral molecule (see **Table 1**) and is 48.7 kJ/mol.

Table 1. Energy effects (ΔH_{298}) of the interaction of epirubicin with fullerene and graphene-like planes (in kJ/mol).

Protolytic form of epirubicin	Adsorbent	
	C60	C54H18
H3A+	−121.3	−209.1
H2A	−38.5	−138.8
HA-	−48.7	−18.7
A2-	−69.4	−35.9

A further increase in the charge of the anion from one to two leads to a change in the intermolecular complex structure of the epirubicin dianion with fullerene (**Figure 5d**), in comparison with the intermolecular complex of the epirubicin monoanion with fullerene (**Figure 4c**) and, as a result, to a change in the interaction enthalpy from −48.7 to −69.4 kJ/mol (see **Table 1**).

The next task was to investigate the interaction of the graphene-like plane with the epirubicin molecule in various protolithic forms. **Figure 6a** shows the intermolecular complex of a graphene-like plane with a protonated form of epirubicin. It can be seen from the figure, the epirubicin cation is placed on the graphene sheet almost parallel to it. In this complex, dispersion interaction occurs with a larger number of atoms of structural units compared to the intermolecular fullerene-cation complex (**Figure 5a**). At the same time, as expected, the calculated enthalpy of intermolecular interaction is significantly higher (−209.1 kJ/mol) compared to the similar value for the complex fullerene—protonated form of epirubicin (−121.3 kJ/mol) (see **Table 1**).

The intermolecular complex obtained as a result of the interaction of a graphene-like plane with a neutral epirubicin molecule (**Figure 6b**) is structurally similar to the complex with an epirubicin cation (**Figure 6a**). Both intermolecular complexes are characterized by a parallel arrangement of the anthraquinone aromatic framework relative to the graphene-like plane. As a result, the enthalpy of intermolecular interaction also has a rather high value, which is –138.8 kJ/mol.

When the mono- and dianion of epirubicin interacts with a graphene-like plane, similar intermolecular complexes are formed (**Figure 6c,d**). Unlike the previous two (**Figure 6a,b**), they are characterized by a non-parallel orientation of the anthraquinone aromatic framework to the graphene-like plane. In this regard, fewer atoms of the reacting molecules interact with each other due to dispersion forces. Therefore, the enthalpies of intermolecular interaction for anions (HA$^-$, A^{2-}) of epirubicin are significantly smaller, compared to similar values for protonated and molecular forms of epirubicin. In particular, the interaction enthalpy for the epirubicin monoanion–graphene-like plane complex is −18.7 kJ/mol, and for the epirubicin dianion—graphene-like plane complex, this value is 17.2 kJ/mol higher and has a value of 35.9 kJ/mol.
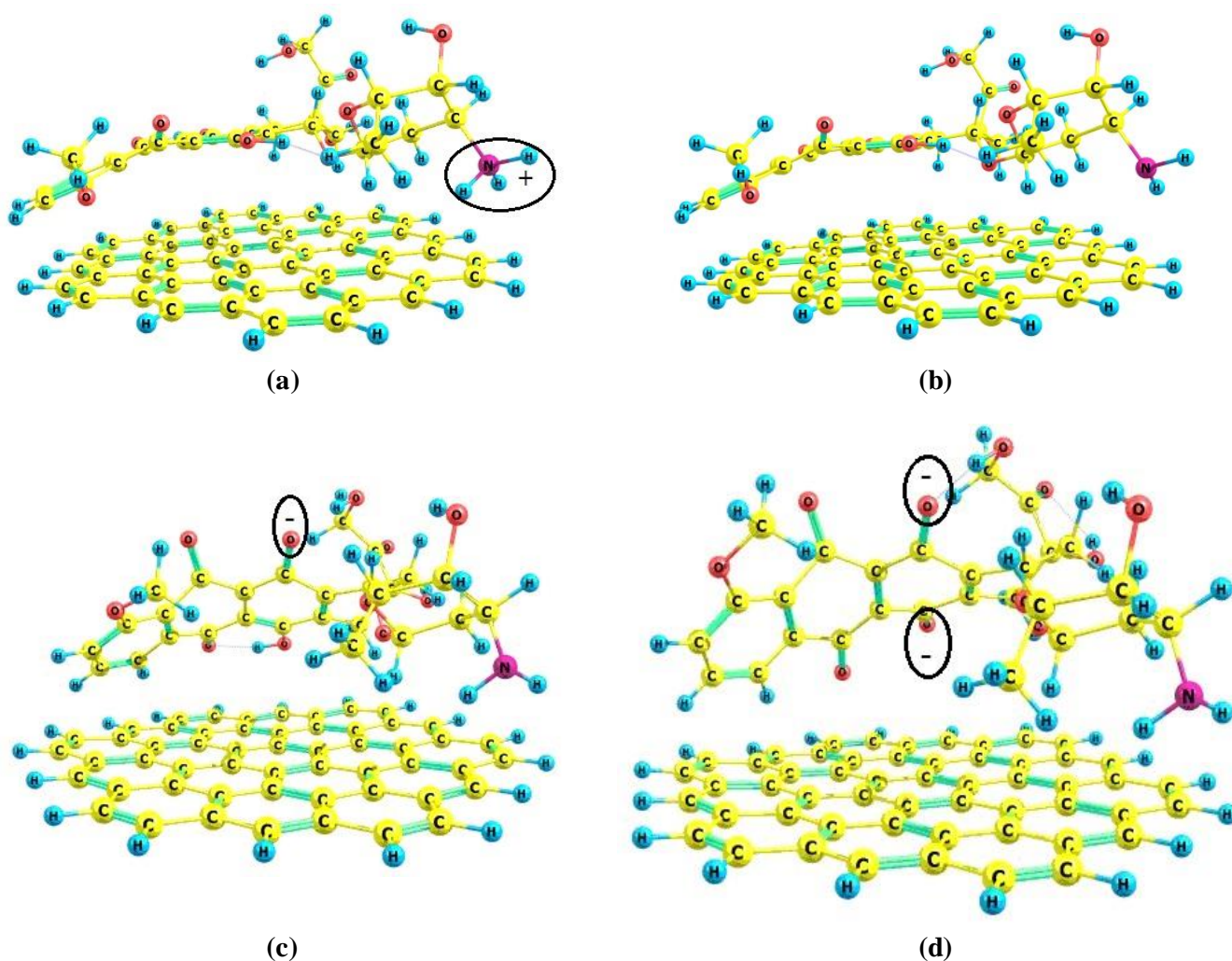
Figure 6. Equilibrium geometry of intermolecular complexes of a graphene-like plane with protolytic forms of epirubicin: **(a)** protonated; (b) neutral epirubicin molecule; **(c)** monodeprotonated; **(d)** dideprotonated.

It can be seen from the table that all values of the enthalpy of intermolecular interaction are negative values, which indicates the thermodynamic probability of adsorption for all considered protolytic forms of epirubicin, both for fullerene and for the graphene-like plane. An analysis of the results of quantum chemical calculations shows (see **Table 1**) that the largest value of ΔH_{298} relative to interaction with both fullerene and a graphene-like plane is characteristic of the protonated form (H_3A^+) of epirubicin and is −121.3 (in the case of fullerene) or −209.1 kJ/mol (in the case of a graphene-like plane).

The lowest value of the enthalpy of intermolecular interaction with fullerene is revealed for the neutral molecule of epirubicin, which is −38.5 kJ/mol, and for interaction with a graphene-like plane—the monodeprotonated form of epirubicin (HA^-) (−18.7 kJ/mol). Such weakly bound states of epirubicin molecules are the most promising dosage forms, since their detachment is not accompanied by intense release of thermal energy. The dependence of the binding energy E_i of epirubicin molecules with carbon and hydrogen atoms of nanocarriers indicates the possibility of E_i value varying during their delivery to desease organ due to adsorption of

functional groups from the environment and the resulting change in the charge density distribution in the electronic spectra of carbon nanocarriers. In addition, the range of E_i value changes is due primarily to variations in the hydrogen bond energy contribution when the epirubicin molecule charge state changes. When penetrating within cells with increased acidity of the intracellular environment and the concentration of hydrogen ions, the processes of drug detachment from the nanocarrier and dissociation of the epirubicin molecule into atomic fragments can be enhanced due to electrostatic interaction with hydrogen ions. The migration of detached epirubicin molecules and their dissociates to the cell nucleus is probably caused to dispersed interactions with fluctuations in the dipole moment of the intracellular environment stimulated by changes in the blood pressure due to contractions of the heart muscle.

4. Conclusions

Based on the analysis of the results of quantum chemical calculations, it was found that the most proton-donating hydroxyl groups of the epirubicin molecule are located on its atraquinone fragment.

The thermodynamic probability of adsorption of epirubicin on GP in the entire pH interval of the aqueous medium is assumed, as evidenced by the negative values of interaction enthalpies in all four cases.

It was found that epirubicin (protonated form) will have the greatest adsorption both on the graphene plane (209.1 kJ/mol) and upon interaction with the fullerene molecule (121.3 kJ/mol).

The lowest value of the enthalpy of intermolecular interaction during interaction with fullerene is characteristic for the neutral molecule of epirubicin (−38.5 kJ/mol), and when interacting with a graphene-like plane—for the monoanion of epirubicin (−18.7 kJ/mol).

Based on the obtained calculation results, it can be predicted that the adsorption of epirubicin on the surface of nanocarbon particles will best occur in an aqueous medium with pH < 7. The application of the results of quantum chemical calculations to intracellular processes is considered.

Author contributions: Working idea, theoretical conceptions of intermolecular and intracellular interactions, BMG; mathematical modeling and quantum chemical calculations, EMD, AGG and VVL; editing manuscript (figures, references etc.), OVK and NAH. All authors have read and agreed to the published version of the manuscript.

Conflict of interest: The authors declare no conflict of interest.

References

1.   Menna P, Gonzalez Paz O, Chello M, et al. Anthracycline cardiotoxicity. Expert Opinion on Drug Safety. 2011; 11(sup1): S21-S36. doi: 10.1517/14740338.2011.589834
2.   Becker MMC, Arruda GFA, Berenguer DRF, et al. Anthracycline cardiotoxicity: current methods of diagnosis and possible role of 18F-FDG PET/CT as a new biomarker. Cardio-Oncology. 2023; 9(1). doi: 10.1186/s40959-023-00161-6

3. Huang J, Wu R, Chen L, et al. Understanding Anthracycline Cardiotoxicity From Mitochondrial Aspect. Frontiers in Pharmacology. 2022; 13. doi: 10.3389/fphar.2022.811406

4. Russo M, Della Sala A, Tocchetti CG, et al. Metabolic Aspects of Anthracycline Cardiotoxicity. Current Treatment Options in Oncology. 2021; 22(2). doi: 10.1007/s11864-020-00812-1

5. Sawicki KT, Sala V, Prever L, et al. Preventing and Treating Anthracycline Cardiotoxicity: New Insights. Annual Review of Pharmacology and Toxicology. 2021; 61(1): 309-332. doi: 10.1146/annurev-pharmtox-030620-104842

6. Cappetta D, Rossi F, Piegari E, et al. Doxorubicin targets multiple players: A new view of an old problem. Pharmacological Research. 2018; 127: 4-14. doi: 10.1016/j.phrs.2017.03.016

7. McGowan JV, Chung R, Maulik A, et al. Anthracycline Chemotherapy and Cardiotoxicity. Cardiovascular Drugs and Therapy. 2017; 31(1): 63-75. doi: 10.1007/s10557-016-6711-0

8. Zhu H, Sarkar S, Scott L, et al. Doxorubicin Redox Biology: Redox Cycling, Topoisomerase Inhibition, and Oxidative Stress. Reactive Oxygen Species. Published online May 2016: 189-198. doi: 10.20455/ros.2016.835

9. Valcovici M, Andrica F, Serban C, et al. Cardiotoxicity of anthracycline therapy: current perspectives. Archives of Medical Science. 2016; 2: 428-435. doi: 10.5114/aoms.2016.59270

10. Pourmadadi M, Farokh A, Rahmani E, et al. Polyacrylic acid mediated targeted drug delivery nano-systems: A review. Journal of Drug Delivery Science and Technology. 2023; 80: 104169. doi: 10.1016/j.jddst.2023.104169

11. Lu Y, Shi Y, Wu Q, et al. An Overview of Drug Delivery Nanosystems for Sepsis-Related Liver Injury Treatment. International Journal of Nanomedicine. 2023; 18: 765-779. doi: 10.2147/ijn.s394802

12. Iravani S, Varma RS. Advanced Drug Delivery Micro- and Nanosystems for Cardiovascular Diseases. Molecules. 2022; 27(18): 5843. doi: 10.3390/molecules27185843

13. Cho K, Wang X, Nie S, et al. Therapeutic Nanoparticles for Drug Delivery in Cancer. Clinical Cancer Research. 2008; 14(5): 1310-1316. doi: 10.1158/1078-0432.ccr-07-1441

14. Liu R, Luo C, Pang Z, et al. Advances of nanoparticles as drug delivery systems for disease diagnosis and treatment. Chinese Chemical Letters. 2023; 34(2): 107518. doi: 10.1016/j.cclet.2022.05.032

15. Fabozzi A, Della Sala F, di Gennaro M, et al. Design of functional nanoparticles by microfluidic platforms as advanced drug delivery systems for cancer therapy. Lab on a Chip. 2023; 23(5): 1389-1409. doi: 10.1039/d2lc00933a

16. Hosseini SM, Mohammadnejad J, Najafi-Taher R, et al. Multifunctional Carbon-Based Nanoparticles: Theranostic Applications in Cancer Therapy and Diagnosis. ACS Applied Bio Materials. 2023; 6(4): 1323-1338. doi: 10.1021/acsabm.2c01000

17. Chen L, Hong W, Duan S, et al. Graphene quantum dots mediated magnetic chitosan drug delivery nanosystems for targeting synergistic photothermal-chemotherapy of hepatocellular carcinoma. Cancer Biology & Therapy. 2022; 23(1): 281-293. doi: 10.1080/15384047.2022.2054249

18. Jampilek J, Kralova K. Advances in Drug Delivery Nanosystems Using Graphene-Based Materials and Carbon Nanotubes. Materials. 2021; 14(5): 1059. doi: 10.3390/ma14051059

19. Anilkumar P, Lu F, Cao L, et al. Fullerenes for Applications in Biology and Medicine. Current Medicinal Chemistry. 2011; 18(14): 2045-2059. doi: 10.2174/092986711795656225

20. Axet MR, Dechy-Cabaret O, Durand J, et al. Coordination chemistry on carbon surfaces. Coordination Chemistry Reviews. 2016; 308: 236-345. doi: 10.1016/j.ccr.2015.06.005

21. Grebinyk A, Prylutska S, Chepurna O, et al. Synergy of Chemo- and Photodynamic Therapies with C60 Fullerene-Doxorubicin Nanocomplex. Nanomaterials. 2019; 9(11): 1540. doi: 10.3390/nano9111540

22. Vovusha H, Banerjee D, Yadav MK, et al. Binding Characteristics of Anticancer Drug Doxorubicin with Two-Dimensional Graphene and Graphene Oxide: Insights from Density Functional Theory Calculations and Fluorescence Spectroscopy. The Journal of Physical Chemistry C. 2018; 122(36): 21031-21038. doi: 10.1021/acs.jpcc.8b04496

23. Petit K, Suwalsky M, Colina JR, et al. Toxic effects of the anticancer drug epirubicin in vitro assayed in human erythrocytes. Toxicology in Vitro. 2020; 68: 104964. doi: 10.1016/j.tiv.2020.104964

24. Luiz MT, Dutra JAP, Di Filippo LD, et al. Epirubicin: Biological Properties, Analytical Methods, and Drug Delivery Nanosystems. Critical Reviews in Analytical Chemistry. 2021; 53(5): 1080-1093. doi: 10.1080/10408347.2021.2007469

25. Launchbury AP, Habboubi N. Epirubicin and doxorubicin: a comparison of their characteristics, therapeutic activity and toxicity. Cancer Treatment Reviews. 1993; 19(3): 197-228. doi: 10.1016/0305-7372(93)90036-Q

26. Anilanmert B, Arioz Ozdemir F, Erdinc N, et al. Potentiometric determination of the dissociation constants of epirubicin HCl and irinotecan HCl. Mendeleev Communications. 2006; 16(2): 97-98. doi: 10.1070/mc2006v016n02abeh002234

27. Zhu S, Yan L, Ji X, et al. Conformational diversity of anthracycline anticancer antibiotics: A density functional theory calculation. Journal of Molecular Structure: THEOCHEM. 2010; 951(1-3): 60-68. doi: 10.1016/j.theochem.2010.04.008

28. Samide A, Tutunaru B, Varut RM, et al. Interactions of Some Chemotherapeutic Agents as Epirubicin, Gemcitabine and Paclitaxel in Multicomponent Systems Based on Orange Essential Oil. Pharmaceuticals. 2021; 14(7): 619. doi: 10.3390/ph14070619

29. Lombardi P, Animati F, Cipollone A, et al. Synthesis and conformational preference of novel 8-fluoroanthracyclines. Acta Biochimica Polonica. 1995; 42(4): 433-444. doi: 10.18388/abp.1995_4897

30. Krätschmer W, Lamb LD, Fostiropoulos K, et al. Solid C60: a new form of carbon. Nature. 1990; 347(6291): 354-358. doi: 10.1038/347354a0

31. Chan B, Kawashima Y, Katouda M, et al. From C60 to Infinity: Large-Scale Quantum Chemistry Calculations of the Heats of Formation of Higher Fullerenes. Journal of the American Chemical Society. 2016; 138(4): 1420-1429. doi: 10.1021/jacs.5b12518

32. Cherniuk OA, Demianenko EM, Terets MI, et al. Study of the mechanism of influence of carbon nanotubes surface chemistry on the mechanical properties of fiberglass. Applied Nanoscience. 2020; 10(12): 4797-4807. doi: 10.1007/s13204-020-01448-1

33. Stewart JJP. MOPAC2016. Stewart Computational Chemistry. Colorado Springs, CO, USA; 2016.

34. Stewart JJP. Optimization of parameters for semiempirical methods V: Modification of NDDO approximations and application to 70 elements. Journal of Molecular Modeling. 2007; 13(12): 1173-1213. doi: 10.1007/s00894-007-0233-4

35. Řezáč J, Hobza P. Advanced Corrections of Hydrogen Bonding and Dispersion for Semiempirical Quantum Mechanical Methods. Journal of Chemical Theory and Computation. 2011; 8(1): 141-151. doi: 10.1021/ct200751e

36. Řezáč J, Riley KE, Hobza P. Benchmark Calculations of Noncovalent Interactions of Halogenated Molecules. Journal of Chemical Theory and Computation. 2012; 8(11): 4285-4292. doi: 10.1021/ct300647k